FEBS Letters 512 (2002) 116–120 FEBS 25726

The first room-temperature X-ray absorption spectra of higher oxidation states of the tetra-manganese complex of photosystem II

Michael Haumann[a,**], Markus Grabolle[a], Thomas Neisius[b], Holger Dau[a,*]

[a] *Fachbereich Physik, Freie Universität Berlin, Arnimallee 14, D-14195 Berlin, Germany*
[b] *European Synchrotron Radiation Facility, BP. 220, 38043 Grenoble Cedex, France*

Received 20 December 2001; accepted 21 December 2001

First published online 18 January 2002

Edited by Richard Cogdell

Abstract The manganese (Mn) complex of photosystem II catalyzes water oxidation. For the first time, its advancement through the reaction cycle was monitored by time-resolved X-ray absorption measurements at the Mn K-edge at room temperature. The complex was stepped through its four oxidation states by nano-second-laser flashes applied to samples exposed to the X-ray beam. Time courses of the X-ray fluorescence intensity were recorded during a flash sequence. Extended X-ray absorption fine-structure spectra were recorded with the S_1, S_2, and S_3 oxidation states highly populated. The room temperature data is compatible with the formation of a third di-μ-oxo bridge between two Mn atoms upon the $S_2 \rightarrow S_3$ transition.

Key words: Bio-X-ray absorption spectroscopy; Metalloenzyme; Photosynthesis; Manganese complex; Oxygen evolution

1. Introduction

Investigation by X-ray absorption spectroscopy (XAS) can provide deeper insights in atomic structure and function of the metal sites of metalloenzymes [1,2]. However, in the past, XAS measurements of proteins mainly have been carried out at cryogenic temperatures. Thereby, the method has been restricted to the analysis of the frozen metal site with the enzyme in potentially ambiguous cryo-conditions (e.g. ill-defined pH, ionic and redox equilibria). A promising new approach for the analysis of dynamics and changes in the metal site of functional enzymes in atomic detail is X-ray spectroscopy on non-crystalline samples at room temperature [12].

Here, we report first results of room-temperature XAS measurements on structural changes of the manganese (Mn) complex of photosystem II (PSII). PSII is a large multi-subunit protein-cofactor complex found in the thylakoid membrane of higher plants and cyanobacteria [3,4]. It catalyzes the light-driven oxidation of two bound water molecules to molecular oxygen, thereby providing most of the oxygen in the atmosphere. The catalytic function of water oxidation takes place at a tetra-nuclear Mn complex, bound at the lumenal side of the D1 subunit of PSII [3–10]. Recently, the crystal structure of PSII has been determined at a resolution of 3.8 Å [5]. Electron densities of the Mn complex have been identified but details of the metal site remain invisible.

Water oxidation by PSII is a five-step process. The absorption of one quantum of light by the enzyme leads to the abstraction of one electron from the Mn complex. By the successive abstraction of four electrons, the Mn complex becomes increasingly oxidized. The formal redox states are named S_0–S_4 [6]. Each abstraction of an electron induces a $S_i \rightarrow S_{i+1}$ transition (S_i: oxidation state of the Mn complex) until, finally, S_4 is reached. Under release of dioxygen, S_4 is rapidly converted to S_0 (without input of light energy), thereby closing the reaction cycle [7]. Previous XAS results on structure and oxidation state of the Mn complex mainly have been obtained at cryogenic temperatures. From these experiments several structural models of the Mn complex have been deduced [8–11]. First XAS results obtained at room temperature, with the Mn complex in its S_1-state, revealed subtle differences between low- and high-temperature structures [12]. Low-temperature XAS measurements point to significant structural changes at the metal site during some of the redox transitions [8,9,13]. So far, these changes are only poorly characterized and understood.

In this work, the redox states are highly enriched by the application of nano-second-laser flashes to the PSII samples exposed to the X-ray beam (at beamline ID26 of the European Synchrotron Radiation Facility (ESRF) Grenoble, France). For the first time, EXAFS spectra for three oxidation states of the manganese complex are obtained at room temperature. We discuss structural changes at the Mn complex during the catalytic cycle of water oxidation.

2. Materials and methods

2.1. PSII-enriched membrane particles

PSII-enriched membrane particles were prepared from market spinach as described in [14,15] and stored at −80°C until use. The oxygen-evolution activity of the preparations under white-light illumination was 1200–1400 μmol O_2/(mg Chl/h) at 28°C [15].

2.2. PSII membrane multilayers

For the preparation of PSII membrane multilayers suitable for X-ray absorption measurements, PSII membrane particles were dissolved at 1 mg/ml of chlorophyll in a medium containing 15 mM NaCl, 5 mM $MgCl_2$, 5 mM $CaCl_2$, 1 M betaine, 10% v/v glycerol, and 25 mM 2-(*N*-morpholino)ethanesulfonic acid, pH 6.2. An artificial electron acceptor, PPBQ, was added to yield a final concentration of 200 μM. Multi-

**Also corresponding author..
*Corresponding author. Fax: (49)-30-8385 6299.
E-mail address: holger.dau@physik.fu-berlin.de (H. Dau).

Abbreviations: EXAFS, extended X-ray absorption fine-structure; FT, Fourier transform; Mn, manganese; PSII, photosystem II; S_i, oxidation state of the Mn complex; XAS, X-ray absorption spectroscopy

0014-5793/02/$22.00
PII: S0014-5793(02)02237-8

layers were then prepared by centrifugation of PSII membranes onto Kapton foil (sample dimensions ca. 15×2 mm) [14,16,17]. The obtained PSII multilayers (thickness ~200 μm) were illuminated from both sides by a single actinic flash from Xenon-flash lamps, dark-adapted and partially dehydrated by drying for 2 h at 4°C in darkness, and then stored in liquid nitrogen. This procedure yielded almost 100% population of the S_1-state. Each sample contained about 0.14 mg of chlorophyll and Mn at a concentration of about 1 mM. The whole preparation was carried out under dim green light.

2.3. X-ray absorption measurements

X-ray absorption measurements were carried out at the undulator beamline ID26 of the ESRF in Grenoble, France. Mn X-ray absorption spectra were measured by monitoring the excited X-ray fluorescence (fluorescence-detected absorption). The spectra were collected by scanning of a Si220 crystal monochromator. The sample was placed in plain air and kept at room temperature. The excitation angle between the electric-field vector of the X-ray beam and the normal to the surface of the PSII multilayers was 45°. X-ray fluorescence was detected perpendicularly to the incident beam by a PIN photodiode (22 mm diameter, Eurisys Meassures). A chromium filter and a thin aluminum foil in front of the photodiode suppressed scattered X-rays and laser light, respectively. Only one scan per sample was performed (X-ray spot size ca. 0.5×0.1 mm, photon flux ~$5\times10^{11}s^{-1}$). In comparison to Meinke et al. [12], the X-ray intensity was here reduced by a factor of about two. For further details see [12,18].

2.4. Laser-flash excitation

Laser-flash excitation of the samples was performed at the beamline ID26 by a frequency-doubled, Q-switched Nd-YAG laser (Quantel Brilliant, FWHM 5 ns, 532 nm, ca. 150 mJ per flash). The laser beam was widened by lenses to a spot size of ca. 20×8 mm. Half of the spot illuminated the front side of the sample directly. The other half was reflected by a mirror to the back-side of the sample. This setup ensured saturating illumination of the sample. The laser flashes and data acquisition were synchronized using appropriate trigger electronics.

2.5. Types of XAS experiments

We performed two types of XAS experiments. (1) Time-scans were carried out at a fixed exciting X-ray energy and the X-ray fluorescence intensity was measured as function of time. A rapid beam shutter (t_{open} ~10 ms) opened about 0.2 s before the start of data collection. (2) Rapid EXAFS scans (scan range 6500–7100 eV) were performed using the rapid-scan mode (synchronous scan of undulator gap and monochromator) of ID26 within 9 s. The data range later used for quantitative evaluation (6500–6906 eV) corresponds to an X-ray exposure time of only 6.2 s. Zero, one, and two laser flashes (spaced by 300 ms) had been applied to the sample, then the rapid beam shutter was opened (0.2 s after the last flash), and data collection started ~0.2 s later (600 points per spectrum, 15 ms per data point).

2.6. Data evaluation

Each EXAFS spectrum represents the average of 20–25 individual scans; each scan was performed on a different sample which was taken from five different batches of samples, each prepared from a different PSII membrane preparation. The energy scale was calibrated using the narrow pre-edge peak of the simultaneously measured $KMnO_4$ absorption as a standard. After subtraction of the pre-edge background, the averaged spectra (20–25 scans) were normalized as in [12,16]. The energy scale of the EXAFS data was transformed to a wave-vector scale (k-scale) using an energy threshold (E_0) of 6546 eV. EXAFS data were averaged to yield data points equally spaced on a k-scale. Spectra were simulated using an amplitude weighting factor of 0.85. Phase functions for different elements in the various shells of backscatterers were calculated using FEFF (see [19], version 7). The k^3-weighted EXAFS spectra were simulated by a least-squares procedure using the in-house software SimX [20].

3. Results and discussion

3.1. Photoreduction of the Mn complex during X-ray irradiation at room temperature

Irradiation of PSII samples with intense X-rays creates numerous radicals per absorbed photon [21], reducing the Mn complex at a rate which strongly depends on temperature [12,21]. We analyzed the reduction of the Mn complex (initially in its S_1-state) by monitoring the change in X-ray fluorescence intensity for excitation at a fixed X-ray energy (6549.5 eV) in the rising region of the Mn K-edge (Fig. 1A). During X-ray irradiation, the fluorescence intensity increases (Fig. 1A) due to the shift of the Mn K-edge to lower energies upon Mn reduction (see inset in Fig. 1A). Starting with an edge shape and energy (6551.7 eV, determined by the 'integral method' [22]) which is typical for the S_1-state [12], after about 6 min of X-ray irradiation the K-edge is down-shifted by 4.5 eV to 6547.2 eV and the shape of the edge indicatives the presence of Mn(II) in the sample [23]. The reduction reveals a small but reproducible lag phase which lasts for ~20 s (arrow in Fig. 1A, see also [12]). During this lag the K-edge energy and shape (not shown) remain essentially constant; the down-shift of the K-edge energy of a sample initially in S_1 is essentially zero.

We found that, at low temperatures, the rate of X-ray photoreduction is by a factor of about two accelerated in samples exposed to one or two flashes of light [20]. To be on the safe side with respect to accelerated X-ray photoreduction in higher S-states, in the following, only data is considered which corresponds to X-ray exposure times of 6.2 s, less than one third of the lag time of 20 s. The absence of photoreduction for PSII samples which partial population of the S_2- and S_3-states is confirmed by the Mn K-edge spectrum obtained for samples exposed to 10 laser flashes (Fig. 1B, inset). The edge position for this spectrum, 6552.2 eV, in a spectrum recorded within 6 s after the end of the 10-flash measurement on the same spot versus 6551.7 eV in the S_1-state is in good agreement with the estimated edge energy for equal population of the four S-states. Any significant X-ray photoreduction of PSII in S_2 and S_3 would have resulted in a lower edge energy. These observations rule out a significant reduction of Mn in S_2 and S_3 during EXAFS scans of 6.2 s duration.

3.2. The stepping of the Mn complex through its oxidation states by laser-flash excitation

In the past, XAS measurements on the Mn complex of PSII in higher oxidation states than S_1 mainly have been performed with samples prepared by a freeze-quench technique: after population of higher S-states by flash or continuous light illumination, the samples had been rapidly frozen and XAS measurements were performed at cryogenic temperatures ([8–10] for review). In the course of the present study we have implemented a new approach: laser-flash excitation of samples exposed to the X-ray beam (at room temperature).

Fig. 1B shows the Mn X-ray fluorescence intensity at a fixed exciting X-ray energy (6551.5 eV, roughly corresponding to the Mn K-edge energy of the S_1-state) as function of time. A train of 10 laser flashes spaced by 500 ms (arrows) was applied to dark-adapted PSII samples. The fluorescence intensity shows a pronounced quartenary oscillation. This effect results from the shift of the Mn K-edge upon each flash originating from the different Mn K-edge energies of the four oxidation states (S_0, S_1, S_2, S_3) of the Mn complex [14,24–26]. Similar oscillations were observed when the spacing between flashes was 300 ms (not shown). The 'sharpness' of the oscillations was found to be significantly increased in comparison to oscillations resulting from illumination of samples with a Xenon-flash lamp (data not shown). The latter effect

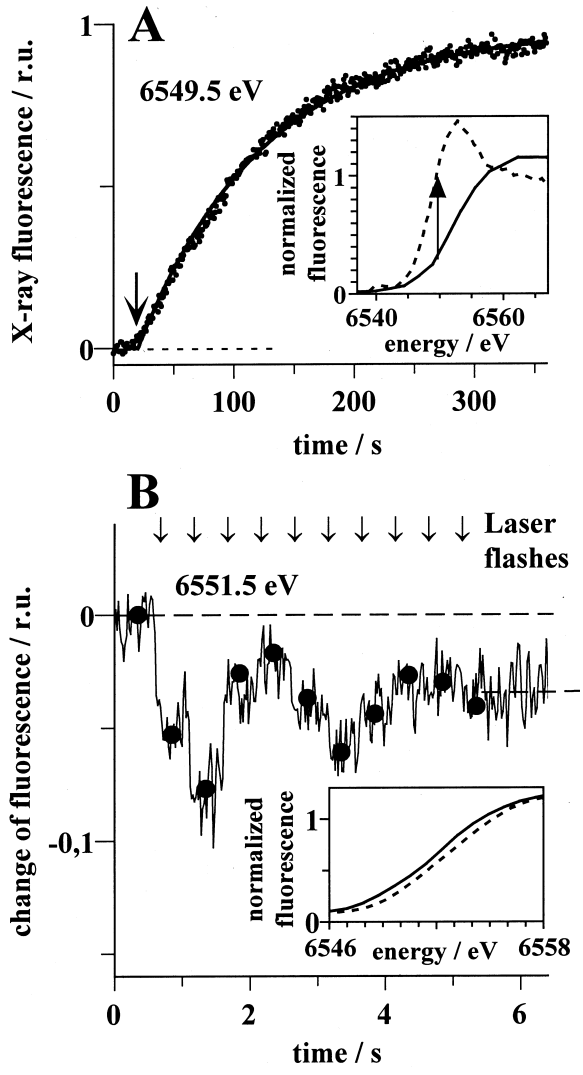

Fig. 1. A: X-ray photoreduction of the Mn complex of PSII (at 291 K) monitored by a time-scan of the X-ray fluorescence intensity at fixed excitation energy (6549.5 eV). The arrow indicates the end of the ~20 s lag phase; the line represents a single-exponential simulation ($k = 0.57$ min^{-1}). Inset: Normalized Mn K-edge spectra after 0.5 s (solid line) and 360 s (dashed line) of X-ray illumination. The arrow indicates the increase in the fluorescence intensity at 6549.5 eV resulting from the down-shift of the K-edge energy. B: Oscillations of X-ray fluorescence intensity at fixed X-ray energy (6551.5 eV) upon illumination of dark-adapted PSII with 10 laser flashes (indicated by arrows). Five traces were averaged; flash-burst artefacts were removed for clarity. The integration time per data point was 15 ms. The dots represent a simulation with parameters given in the text. The dashed lines indicate the fluorescence levels before flashes (S_1-state) and for about equally populated S-states (after 10 flashes). Inset: Normalized Mn K-edge spectra before application of flashes (solid line) and recorded on the same spot after the end of the 10-flash measurement (dashed line).

is attributable to the much shorter (no 'double hits') and more intense (less 'misses') laser flashes used in this work. The oscillations are well simulated (Fig. 1B, circles) under the assumption that 100% of centers were in the S_1-state prior to the first flash, with 14% of 'misses' (per flash 14% of all PSII do not advance in the S-state cycle), and using relative fluorescence changes of 0.63 (transition $S_0 \rightarrow S_2$), 1.0 ($S_1 \rightarrow S_2$), and 0.63 ($S_2 \rightarrow S_3$). It should be noted that the relative fluorescence changes upon flashes can not be directly translated into the K-edge energy shifts upon the S-transitions, because the former are only obtained at a single X-ray energy and the shape of the K-edge differs between S-states [8,14,24–26]. To obtain a lower limit for the population of the S_3-state (worst-case scenario) we also assumed an extra contribution of 15% of centers undergoing only transition $S_1 \rightarrow S_2$ (on the first flash), often observed due to acceptor side limitations [27]. The miss parameter is in the range commonly found in flash spectroscopy on PSII membrane particles [28,29]. Varying the relative fluorescence changes of the individual S-transitions in the simulation did not result in a greatly changed miss parameter (±2%). We calculated the following populations of S-states (taking into account 15% of centers turning over only once), starting with 100% of centers in S_1: S_2, one flash, 86%; S_3, two flashes, 61%. The population of centers in S_3 after two flashes is considered as the lower limit. We conclude that a sufficiently high enrichment of S_1, S_2, and S_3 has been achieved to detect evidence for structural changes by EXAFS analysis (see next section).

3.3. First room-temperature EXAFS spectra of S_1, S_2, and S_3

Dark-adapted PSII samples (S_1-state) were illuminated at room temperature by zero, one, and two laser flashes (spacing 300 ms). Flashes were applied prior to X-ray irradiation, a rapid beam shutter was opened 0.2 s after the last flash, and data collection started 0.2 s thereafter. Fig. 2 shows the k^3-weighted EXAFS oscillations (inset, thin lines) and the corresponding Fourier transforms (FTs).

The EXAFS is related to the backscattering of electrons released from the X-ray absorbing (Mn) by ligands of the first few coordination spheres. Peaks in the Fourier-transformed EXAFS spectrum correspond to 'backscattering' li-

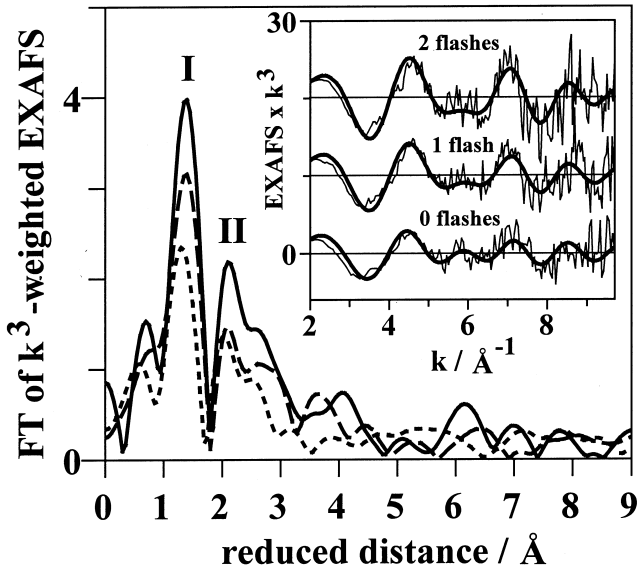

Fig. 2. FTs of normalized k^3-weighted EXAFS oscillations of PSII illuminated by zero, one, and two laser flashes (S_1, S_2, and S_3 predominantly populated) at room temperature. The FTs were calculated for data points ranging from 20 to 360 eV above E_0 (6546 eV) using fractional cosine windows extending over 10% and 20% of the used k-range at low and high k-values, respectively. Short-dashed line, zero flash; dashed line, one flash; solid line, two flashes. Inset: The respective k^3-weighted EXAFS oscillations. Thin lines, experimental data; thick lines, simulations (parameters listed in Table 1). Spectra are drawn on the same scale and vertically displaced for clarity.

Table 1
Parameters of EXAFS spectra of the Mn complex after zero, one, and two laser flashes (S_1, S_2, and S_3 predominantly populated)

Shell, N_i	Vector	Coordination number, N_i[per Mn]	Distance, R_i[Å]	Debye–Waller parameter, $2\sigma^2$[Å^2]
		zero/one/two flashes		
I	Mn–O/N	5.5	1.88/1.87/1.86	0.064/0.042/0.030
II	Mn–Mn	0.93/1.05/1.41	2.71/2.71/2.72	0.012

Simulations were carried out for k^3-weighted EXAFS oscillation with k ranging from 20 to 360 eV above E_0 (6546 eV). N_1 was fixed at a chemically reasonable number of 5.5, $2\sigma_{II}^2$ was coupled to yield equal values for the three spectra. The overall R_F-factor of the simulation of the three spectra was 29%. The R_F factor is equal to the mean deviation between simulated and experimental curves for EXAFS oscillations [8], here corresponding to reduced distances ranging from 1.0 to 2.3 Å.

gands of Mn at a Mn-ligand distance which is by about 0.4 Å greater than the 'reduced' distance in Fig. 2. The FT of the S_1-state spectrum (no flash illumination, short-dashed line) exhibits two major peaks (Fig. 2). Peak I is attributed to the O/N ligands of the first coordination sphere of Mn. It increases upon the first flash (S_2-state predominantly populated, dashed line) and, again, upon the second flash (S_3-state predominantly populated, solid line). Presumably, this behavior reflects the oxidation of the Mn complex from $Mn(III)_2Mn(IV)_2$ to $Mn(IV)_4$. (Since the Mn-ligand distances differ between Mn(IV) ligands and Mn(III) ligands, in the $Mn(IV)_4$ complex the distance distribution is, most likely, more homogeneous. Consequently, destructive interference of EXAFS oscillations is reduced and the FT peak is increased in the $Mn(IV)_4$ complex.) Peak II is attributed to EXAFS interactions between heavy atoms, mainly 2.7 Å Mn-Mn interactions [8–10,30]. Peak II is not significantly changed upon the application of the first flash (S_2 formation). Upon formation of S_3 in the majority of PSII (after two flashes, solid line), however, the peak amplitude increases significantly. Noteworthy, the increase in the EXAFS oscillations corresponding to Peak II is too pronounced to be explainable by noise contributions.

Comparing the new room-temperature results and our previously obtained 20 K results (flash-freeze approach, [8,31]) we observe a similar behavior. Specifically, the increase of peak II upon the $S_2 \rightarrow S_3$ transition is observed at both temperatures (different results have been published by other authors [32,35]). Peak II in the S_1-state has been attributed to two to three 2.7 Å Mn–Mn EXAFS interactions which are attributed to two to three di-μ-oxo-bridged pairs of Mn atoms [8–10]. Experiments where two Mn atoms are simultaneously released from the center [23,33] suggest that there are two di-μ-oxo-bridged Mn pairs. A straightforward interpretation of the increase of peak II in the spectrum obtained after two flashes is the formation of a third di-μ-oxo bridge in the S_3-state [8,31,34].

Taking into consideration the relatively high noise level, we have simulated the EXAFS oscillations in Fig. 2 (inset) using only two shells of backscatterers, one shell of light atoms (O/N) and one shell of heavy atoms (Mn). Only the k^3-weighted k-space data was subjected to curve-fitting. The simulation curves are shown in the inset of Fig. 2 (thick lines); the simulation parameters are listed in Table 1. The three spectra differ clearly and all the major differences are well reproduced by the simulations. The fit results are compatible with the existence of two di-μ-oxo bridges in S_1 and S_2 (two Mn–Mn distances of $\sim$2.7 Å resulting in a coordination number of $N_{II} \sim 1$) and of three di-μ-oxo bridges in S_3 (three Mn–Mn distances of $\sim$2.7 Å, $N_{II} \sim 1.5$), respectively.

4. Conclusions

We report the very first room-temperature XAS results obtained for single-turnover nanosecondlaser-flash excitation of PSII samples at the X-ray beamline. Mn EXAFS spectra were recorded within 6.2 s for dark-adapted samples with Mn in the S_1-state and after application of one and two laser flashes (predominant population of the S_2- and S_3-state). The S-state dependence of the EXAFS spectra collected at room temperature is similar to the one observed at 20 K [8,31]. The difference between the EXAFS spectra observed after illumination with one and two laser flashes is compatible with the formation of a third di-μ-oxo bridge upon the $S_2 \rightarrow S_3$ transition, but incompatible with the recently proposed absence of Mn–Mn distances below 2.8 Å in S_3 [35]. Future improvement of the time resolution of the experiment should allow for 'real-time' investigation of the structural changes during the catalytic cycle of water oxidation which occur immediately after the initiating laser flash.

Acknowledgements: We gratefully acknowledge financial support by the German BMBF in the program 'Erforschung kondensierter Materie' (Grant 05KS1KEA/6) and from the Deutsche Forschungsgemeinschaft (SFB 498/C6). We thank the ESRF and specifically the staff of beamline ID26 for excellent support.

References

[1] Teo, B.K. (1986) EXAFS: Basic Principles and Data Analysis, Springer Verlag, Berlin.
[2] Scott, R.A. (2000) in: Physical Methods in Bioinorganic Chemistry – Spectroscopy and Magnetism (Que, L., Ed.), pp. 465–504, University Science Books, Sausalito.
[3] Renger, G. (2001) Biochim. Biophys. Acta 1503, 210–228.
[4] Debus, R.J. (1992) Biochim. Biophys. Acta 1102, 269–352.
[5] Zouni, A., Witt, H.-T., Kern, J., Fromme, P., Krauß, N., Saenger, W. and Orth, P. (2001) Nature 409, 739–743.
[6] Kok, B., Forbush, B. and McGloin, M. (1970) Photochem. Photobiol. 11, 457–475.
[7] Haumann, M. and Junge, W. (1999) Biochim. Biophys. Acta 1411, 86–91.
[8] Dau, H., Iuzzolino, L. and Dittmer, J. (2001) Biochim. Biophys. Acta 1503, 24–39.
[9] Robblee, J., Cinco, R. and Yachandra, V.K. (2001) Biochim. Biophys. Acta 1503, 15–23.
[10] Penner-Hahn, J.E. (1998) Struct. Bonding 90, 1–36.
[11] MacLachlan, D.J., Nugent, J.H.A. and Evans, M.C.W. (1994) Biochim. Biophys. Acta 1185, 103–111.
[12] Meinke, C., Sole, A.V., Pospisil, P. and Dau, H. (2000) Biochemistry 39, 7033–7040.
[13] Messinger, J. (2000) Biochim. Biophys. Acta 1459, 481–488.
[14] Iuzzolino, L., Dittmer, J., Doerner, W., Meyer-Klaucke, W. and Dau, H. (1998) Biochemistry 37, 17112–17119.
[15] Schiller, H. and Dau, H. (2000) J. Photochem. Photobiol. B Biol. 55, 138–144.
[16] Schiller, H., Dittmer, J., Iuzzolino, L., Dörner, W., Meyer-

Klaucke, W., Sole, V.A., Nolting, H.-F. and Dau, H. (1998) Biochemistry 37, 7340–7350.
[17] Dittmer, J. and Dau, H. (1998) J. Phys. Chem. 102, 8196–8200.
[18] Sole, V.A., Gauthier, C., Signorato, R., Goulon, J. and Moguiline, E.J.J. (1999) Synchrotron Rad. 6, 164–166.
[19] Rehr, J., Mustre de Leon, J., Zabinsky, S.I. and Albers, R.C. (1991) J. Am. Chem. Soc. 113, 5135.
[20] Dittmer, J. (1999) Ph.D. Thesis, Christian Albrechts Universität, Kiel.
[21] Dau, H., Dittmer, J., Iuzzolino, L., Schiller, H., Dörner, W., Heinze, I., Sole, V.A. and Nolting, H.-F. (1997) J. Phys. IV, 607–610.
[22] Dittmer, J., Iuzzolino, L., Dörner, W., Nolting, H.-F., Meyer-Klaucke, W. and Dau, H. (1998) in: Photosynthesis: Mechanism and Effects (Garab, G., Ed.), pp. 1339–1342, Kluwer Academic Publishers, Dordrecht.
[23] Pospisil, P., Haumann, M., Dittmer, J., Sole, A. and Dau, H. (2001) Proceedings of the 12th International Congress on Photosynthesis, CSIRO Publishing, Brisbane, in press.
[24] Roelofs, T.A., Liang, W., Latimer, M.J., Cinco, R., Rompel, A., Andrews, J.C., Sauer, K., Yachandra, V.K. and Klein, M.P. (1996) Proc. Natl. Acad. Sci. USA 93, 3335–3340.
[25] Ono, T., Noguchi, T., Inoue, Y., Kusunoki, M., Matsushita, T. and Oyanagi, H. (1992) Science 258, 1335–1337.
[26] Messinger, J., Robblee, J.H., Bergmann, U., Fernandez, C., Glatzel, P., Visser, H., Cinco, R.M., McFarlane, K.L., Bellacchio, E., Pizarro, S.A., Cramer, S.P., Sauer, K., Klein, M.P. and Yachandra, V.K. (2001) J. Am. Chem. Soc. 123, 7804–7820.
[27] Lavergne, J. and Briantais, J.-M. (1996) in: Oxygenic Photosynthesis: The Light Reactions (Ort, D. and Yocum, C., Eds.), pp. 265–287, Kluwer Academic Publishers, Dordrecht.
[28] Karge, M., Irrgang, K.-D. and Renger, G. (1997) Biochemistry 36, 8904–8913.
[29] Haumann, M., Hundelt, M., Jahns, P., Chroni, S., Bögershausen, O., Ghanotakis, D. and Junge, W. (1997) FEBS Lett. 410, 243–248.
[30] Kirby, J.A., Goodin, D.B., Wydrzynski, T., Robertson, A.S. and Klein, M.P. (1981) J. Am. Chem. Soc. 103, 5537–5542.
[31] Dau, H., Iuzzolino, L., Dittmer, J., Dörner, W., Meyer-Klaucke, W. (1998) in: Photosynthesis: Mechanisms and Effects (Garab, G., Ed.), pp. 1327–1330, Kluwer Academic Publishers, Dordrecht.
[32] Guiles, R.D., Zimmermann, J.L., McDermott, A.E., Yachandra, V.K., Cole, J.L., Dexheimer, S.L., Britt, R.D., Wieghardt, K., Bossek, U., Sauer, K. and Klein, M.P. (1990) Biochemistry 29, 471–485.
[33] Dörner, W., Dittmer, J., Iuzzolino, L. and Dau, H. (1998) in: Photosynthesis: Mechanism and Effects (Garab, G., Ed.), Vol. II, pp. 1343–1346, Kluwer Academic Publishers, Dordrecht.
[34] Haumann, M., Grabolle, M., Werthammer, M., Iuzzolino, L., Dittmer, J., Meyer-Klaucke, W., Neisius, T. and Dau, H. (2001) Proceedings of the 12th International Congress on Photosynthesis, CSIRO Publishing, Brisbane, in press.
[35] Liang, W., Roelofs, T., Cinco, R., Rompel, A., Latimer, M.J., Yu, W., Sauer, K., Klein, M.P. and Yachandra, V.K. (2000) J. Am. Chem. Soc. 122, 3399–3412.